



## Pharmaceutical Biotechnology

# Evaluation of Hydrogen Exchange Mass Spectrometry as a Stability-Indicating Method for Formulation Excipient Screening for an IgG4 Monoclonal Antibody



Ronald T. Toth IV<sup>1</sup>, Samantha E. Pace<sup>1</sup>, Brittney J. Mills<sup>1</sup>, Sangeeta B. Joshi<sup>1</sup>,  
Reza Esfandiary<sup>2</sup>, C. Russell Middaugh<sup>1</sup>, David D. Weis<sup>3,\*</sup>, David B. Volkin<sup>1,\*</sup>

<sup>1</sup> Department of Pharmaceutical Chemistry, Macromolecule and Vaccine Stabilization Center, University of Kansas, 2030 Becker Drive, Lawrence, Kansas 66047

<sup>2</sup> Department of Formulation Sciences, MedImmune LLC, Gaithersburg, Maryland 20878

<sup>3</sup> Department of Chemistry, University of Kansas, 1251 Wescoe Hall Dr, Lawrence, Kansas 66045

## ARTICLE INFO

## Article history:

Received 10 July 2017

Revised 25 October 2017

Accepted 6 December 2017

Available online 18 December 2017

## Keywords:

formulation  
stability  
excipients  
antibodies  
hydrogen exchange  
mass spectrometry

## ABSTRACT

Antibodies are molecules that exhibit diverse conformational changes on different timescales, and there is ongoing interest to better understand the relationship between antibody conformational dynamics and storage stability. Physical stability data for an IgG4 monoclonal antibody (mAb-D) were gathered through traditional forced degradation (temperature and stirring stresses) and accelerated stability studies, in the presence of different additives and solution conditions, as measured by differential scanning calorimetry, size exclusion chromatography, and microflow imaging. The results were correlated with hydrogen exchange mass spectrometry (HX-MS) data gathered for mAb-D in the same formulations. Certain parameters of the HX-MS data, including hydrogen exchange in specific peptide segments in the C<sub>H2</sub> domain, were found to correlate with stabilization and destabilization of additives on mAb-D during thermal stress. No such correlations between mAb physical stability and HX-MS readouts were observed under agitation stress. These results demonstrate that HX-MS can be set up as a streamlined methodology (using minimal material and focusing on key peptide segments at key time points) to screen excipients for their ability to physically stabilize mAbs. However, useful correlations between HX-MS and either accelerated or real-time stability studies will be dependent on a particular mAb's degradation pathway(s) and the type of stresses used.

© 2018 American Pharmacists Association<sup>®</sup>. Published by Elsevier Inc. All rights reserved.

## Introduction

Monoclonal antibodies (mAbs) are an important class of therapeutic biomolecules and represent the majority of protein-based drug candidates currently in development.<sup>1,2</sup> They are molecules that exhibit diverse conformational changes on a variety of timescales, and it is important from a pharmaceutical perspective to better understand the relationship between mAb conformational

stability, conformational dynamics, and storage stability.<sup>3,4</sup> A monoclonal antibody consists of 4 polypeptide chains connected by disulfide bonds, 2 heavy chains, and 2 light chains. The heavy chains form the tertiary structural domains C<sub>H1</sub>, C<sub>H2</sub>, C<sub>H3</sub>, and V<sub>H</sub>, whereas the light chains form the tertiary structural domains C<sub>L</sub> and V<sub>L</sub>.<sup>5</sup> The higher order structure of a mAb consists of 2 antigen-binding domains (Fab) and 1 crystalizable domain (Fc). These structural elements are arranged in a “Y-shaped” structure, with the linkages between domains being highly flexible.<sup>6-8</sup> Owing to the flexible linker, mAbs are highly dynamic molecules in solution, capable of movements ranging from small-scale fluctuations to large-scale rearrangements of the domains.<sup>7-9</sup>

The physicochemical stability of mAbs is a critical factor to consider in the effort to develop high-quality efficacious drug candidates. A common strategy to improve long-term storage stability and to help protect protein pharmaceuticals from environmental stresses is to add one or more excipients to the formulation.

Current address for Dr. Toth: GSK Vaccines, 14200 Shady Grove Rd, Rockville, MD 20850; for Dr. Mills: AbbVie, 1 N Waukegan Road, North Chicago, IL 60064.

This article contains supplementary material available from the authors by request or via the Internet at <https://doi.org/10.1016/j.xphs.2017.12.009>.

\* Correspondence to: David B. Volkin (Telephone: +1-785-864-6262; Fax: +1-785-864-5736) and David D. Weis (Telephone: +1-785-864-1377; Fax: +1-785-864-5396).

E-mail addresses: [volkin@ku.edu](mailto:volkin@ku.edu) (D.B. Volkin), [dweis@ku.edu](mailto:dweis@ku.edu) (D.D. Weis).

<https://doi.org/10.1016/j.xphs.2017.12.009>

0022-3549/© 2018 American Pharmacists Association<sup>®</sup>. Published by Elsevier Inc. All rights reserved.

Some commonly used excipients are salts, amino acids, carboxylic acids, carbohydrates, detergents, sugars, and polyols.<sup>10</sup> Stabilizing excipients are generally identified through excipient screening, an empirical approach where physicochemical stability of the protein of interest is assessed in a large number of test formulations containing excipients of interest. Owing to the large numbers of test formulations, such physical stability profiles are often measured rapidly by taking advantage of high-throughput screening methods employing multiple monitoring techniques.<sup>11–13</sup>

Previous studies in our laboratory have explored the interrelationships between mAb conformational dynamics as measured by hydrogen exchange mass spectrometry (HX-MS), mAb aggregation propensity and conformational stability, and the influence of various pharmaceutical excipients and other additives on each of these parameters. Similarly, the potential and utility for HX-MS to probe for mAb conformational dynamics in pharmaceutical formulations was recently reviewed.<sup>4</sup> It has been shown that backbone dynamics can be significantly altered in specific regions of different mAbs due to varying solution conditions, site-directed mutations, and chemical modifications. In addition, other studies have successfully used HX-MS to characterize aggregation pathways<sup>14</sup> and propensity,<sup>15</sup> and to characterize higher order structural differences resulting from point mutations<sup>16</sup> or between biophysically similar molecules.<sup>17</sup> It has been shown that increased conformational stability and reduced aggregation propensity correlate with small decreases globally in relative local flexibility. In addition, large increases in relative local flexibility in the C<sub>H</sub>2 domain, HC 241–251, correlated with decreased conformational stability and increased aggregation across several different IgG1 mAbs. The ability of HX-MS to monitor backbone dynamics in differing formulations has thus been proposed to be a potential analytical tool for formulation scientists. As opposed to conducting accelerated and real-time stability studies where results take months to years to generate, HX-MS could potentially be used to rapidly assess (using minimal material) rigidifications or perturbations in protein structure in the presence of excipients that correlate with stabilization/destabilization effects observed over time in storage stability studies.

To further expand this idea using a case study, HX-MS was used in this work to monitor conformational dynamics of an IgG4 mAb (mAb-D) in the presence of various additives, including pharmaceutical excipients as well as known protein destabilizers (used as controls), and the results were correlated with traditional biophysical techniques. To the best of our knowledge, this report is the first-time HX-MS with an IgG4 mAb that has been performed in the context of formulation development. In addition, although HX-MS has the potential to be an important tool for excipient screening, one barrier to implementing this approach is that differing excipient solutions can alter chemical exchange rates in hydrogen exchange (HX) experiments, rendering HX results from differing formulations difficult to interpret due to combined effects of additives on the protein's conformational flexibility as well as the inherent chemical exchange rate. Recently, we have validated a procedure to correct HX-MS data for these differences with minimal additional experimentation.<sup>18</sup> To more extensively evaluate the potential applicability of HX-MS for excipient screening as part of the formulation development of therapeutic mAb candidates, the effect of various additives on an IgG4 mAb (mAb-D) was evaluated using traditional approaches with standard biophysical techniques: forced degradation study using DSC (conformational stability), and accelerated stability studies using size exclusion chromatography (SEC) and microflow imaging (MFI; to monitor aggregation and particle formation, respectively). The results from the biophysical measurements are compared with those obtained from HX-MS (using a streamlined version of the methodology) to determine if correlations can be

drawn between the effects of the additives on mAb-D stability as detected by the different approaches/methods.

## Materials and Methods

### Materials

The IgG4 (mAb-D, ~145,000 Da, calculated pI 7.07) was provided by MedImmune (Gaithersburg, MD) at a concentration of 50 mg/mL in 50-mM acetate, 100-mM NaCl, pH 5.5. After dialysis, the mAb concentration was quantified with an Agilent 8453 UV-visible spectrophotometer (Palo Alto, CA). Triplicate samples were prepared by diluting the stock mAb solution 1:50 into buffer. The intensity at 280 nm was averaged for over triplicate analyses. An extinction coefficient of  $1.68 \text{ (mg/mL)}^{-1} \text{ cm}^{-1}$  was used to calculate the protein concentration. Trehalose dihydrate was purchased from Pfanstiehl (Waukegan, IL). Arginine monohydrochloride, deuterium oxide (99 + %D), D-methionine, D-mannitol, porcine pepsin, sodium sulfate, TWEEN<sup>®</sup> 20, and liquid chromatography grade acetic acid and phosphoric acid were purchased from Sigma-Aldrich (St. Louis, MO). Premium grade tris (2-carboxyethyl) phosphine hydrochloride and liquid chromatography-mass spectrometry (LC-MS)-grade formic acid (+99%) were purchased from Thermo Scientific (Rockford, IL). Sodium phosphate dibasic (anhydrous), citric acid (anhydrous), and sodium thiocyanate were purchased from Acros Organics (Fair Lawn, NJ). Sodium chloride, guanidine hydrochloride (Gdn-HCl), LC-MS grade water, acetonitrile, and isopropanol were purchased from Fisher Scientific (Fair Lawn, NJ). For stability studies, glass vials used were from West Pharmaceuticals, (3-mL Vial, Fiolax Clear, Item#6800-0316), and the rubber stoppers were from West Pharmaceuticals (V-35 4432/gray, Item#10122128).

### Sample Preparation

Stock solutions of mAb-D were dialyzed into 5-mM citrate-phosphate (CP) buffer at pH 6.5 or 7.4, with or without 150-mM NaCl. Dialysis was performed using Slide-A-Lyzer cassettes (30,000 MWCO; Thermo Fisher Scientific, Waltham, MA) with a ratio of sample to dialysate at least 1:500, 3 times with at least 4 h between buffer changes. A stock solution of each additive was also prepared in 5-mM CP at pH 6.5 or 7.4, with or without NaCl, at a higher concentration than desired in the final sample. The mAb-D stock solution was diluted using the corresponding CP buffer and the appropriate additive stock solution to achieve a protein concentration of 5 mg/mL and the desired additive concentration (e.g., 0.3-M arginine, 0.3-M guanidine, 0.3-M sodium thiocyanate, 0.3-M sodium sulfate, 0.2-M methionine, 0.4-M trehalose, 0.8-M mannitol, or 0.05% polysorbate 20 [PS20]). Control samples of mAb-D were prepared using only CP buffer at the appropriate pH, with or without NaCl. After addition of mAb-D and the additive, the pH value of the samples was adjusted (using acid and base) to be within 0.1 pH unit of the desired pH. Buffer controls were also prepared in the same manner without addition of mAb-D. Both mAb-D and buffer control samples were placed in a laminar flow hood and sterile filtered using 0.22- $\mu\text{m}$  syringe filters (Millipore, Billerica, MA). Aliquots, 1.5 mL, were placed into 3-mL type I borosilicate glass vials and capped with rubber stoppers and an aluminum overseal (West Pharmaceutical Services, Exton, PA). Before use, glass vials were autoclaved in a large beaker and allowed to cool overnight.

For accelerated stability studies, samples of mAb-D were stored at 4°C and 50°C. Triplicate samples from 3 separate vials were analyzed by SEC and MFI at time 0 and after storage for 2 weeks at 4°C and after 1 and 2 weeks at 50°C. Triplicate buffer samples were prepared and analyzed at time 0 by MFI. For stirring stress studies,

mAb-D and buffer control samples were stressed by placing a small pivot-ring-free stir bar ( $7 \times 2$  mm flea micro; Bel-Art–SP Scienceware, Wayne, NJ) inside each 3-mL vial prepared as described above and stirring on setting 5 at  $25^\circ\text{C}$  for 30 min using a Reacti-Therm III (Thermo Scientific). No vortex was observed under these conditions.

For the HX-MS studies, additives which contain exchangeable hydrogens were fully deuterated before sample preparation. Each additive was prepared in  $\text{D}_2\text{O}$  at a slightly higher than final concentration (to account for dilution effects) and allowed to incubate for 30 min. The additive solution was vacuum dried at  $30^\circ\text{C}$  for 48 h. Two additional cycles of dissolution in  $\text{D}_2\text{O}$  followed by evaporation were performed. The final powder was dissolved in the appropriate volume of CP buffer prepared using  $\text{D}_2\text{O}$ . The pD was adjusted 6.5 or 7.4 with deuterium chloride or deuterium oxide. To account for the offset associated with measuring pD with a pH meter, solutions were adjusted to a pH 0.4 units lower than the desired value.<sup>19</sup>

### Analytical Methods

#### Size Exclusion Chromatography

SEC was performed on all samples using a  $7.8 \text{ mm} \times 30 \text{ cm}$  TOSOH TSK-Gel BioAssist G3SWXL column and  $6.0 \text{ mm ID} \times 4.0 \text{ cm}$  TSK-Gel SWXL guard column (TOSOH Biosciences, King of Prussia, PA), with UV detection at 214 and 280 nm using a prominence high-performance liquid chromatography system (Shimadzu, Tokyo, Japan) equipped with a photodiode array detector. Before analysis, the column was pre-equilibrated with 90 mL of mobile phase, composed of 0.2-M sodium phosphate, pH 6.8. Removal of insoluble aggregates from the stressed samples was accomplished by centrifugation at  $14,000 \times g$  for 5 min before injection onto the column. Molecular weight standards (Biorad Laboratories, Hercules, CA) were used to assess the efficiency of separation. Peaks corresponding to aggregates, monomer, and fragments were selected and quantified using the LC Solutions data analysis package (Shimadzu).

#### Microflow Imaging

A DPA-4200 MFI system (Protein Simple, Santa Clara, CA) was used to count and image subvisible particles in the size range of 2–100  $\mu\text{m}$ . The instrument was calibrated using 10- $\mu\text{m}$  polystyrene particle standards (Duke Standards; Thermo Fisher Scientific, Waltham, MA) before measurements. Measurements were made in triplicate at ambient temperature for all samples with no centrifugation before analysis. The cell was flushed with particle-free water and illumination was optimized using particle-free water before all measurements. The samples were carefully drawn up in a low protein binding, filter-tip pipette (Neptune Scientific) and analyzed using a flow rate of 0.2 mL/min. The purge volume for each measurement was 0.4 and 0.6 mL of sample was analyzed. Particles with circularity greater than 0.95 were filtered out before analysis to avoid counting air bubbles as protein particles.

#### Differential Scanning Calorimetry

Differential scanning calorimetry was performed using a Microcal VP-Capillary DSC equipped with an autosampler (MicroCal, Northampton, MA). Samples were heated from  $15^\circ\text{C}$  to  $85^\circ\text{C}$  using a scan rate of  $1^\circ\text{C}/\text{min}$ . Reference thermograms of buffer containing the respective additives were subtracted from the thermograms of mAb-D in the presence of the additive. Each mAb-D sample was analyzed in triplicate, except mAb-D prepared in Mannitol without NaCl at pH 7.4 in which only 1 and 2 thermograms were used for analysis, respectively. The data were fitted to a multistate model with 2 transitions using the MicroCal LLC DSC plug-in for the Origin

7.0 software. The onset temperature ( $T_{\text{onset}}$ ) was determined using the temperature at which the heat capacity ( $C_p$ ) reached  $500 \text{ cal mol}^{-1} \text{ }^\circ\text{C}^{-1}$  for the first thermal transition.

#### Hydrogen Exchange Mass Spectrometry

HX-MS experiments were performed using a QTOF mass spectrometer (Agilent 6530, Santa Clara, CA) as described previously.<sup>20</sup> Three microliters of mAb-D prepared at 40 mg/mL were labeled with deuterium at  $25^\circ\text{C}$  using 21  $\mu\text{L}$  of deuterated buffer. The pD of all labeling buffers was adjusted to 6.5 or 7.4 with deuterium chloride or deuterium oxide, using the offset associated with measuring pD with a pH meter, solutions were adjusted to a pH 0.4 units lower than the desired value.<sup>19</sup> Samples of mAb-D were subjected to the exchange conditions for either 1000 s (pH 6.5) or 125 s (pH 7.4). Incubation at each time point was completed in triplicate. After incubation, the HX reaction was quenched using a 1:1 dilution into quench buffer (4-M Gdn-HCl, 0.2-M phosphate, 0.5-M tris (2-carboxyethyl) phosphine hydrochloride, pH 2.5) at  $1^\circ\text{C}$  for 60 s. Twenty-five microliters of quenched mAb-D was injected into the sample loop of a refrigerated compartment (maintained at  $0^\circ\text{C}$ ) containing a pepsin column ( $50 \times 2.1 \text{ mm}$ , pepsin was immobilized and packed as described previously<sup>4</sup>), reversed phase trap (Poroshell 120 EC-C8,  $2.1 \times 5 \text{ mm}$ , 2.7 micron particle diameter; Agilent), and reversed phase column (Zorbax 300SB-C18  $2.1 \times 50 \text{ mm}$ , 1.8 micron particle diameter; Agilent).

MS/MS analysis was used to generate a peptide map of mAb-D consisting of 360 peptides with 97% sequence coverage of the light chain and 98% sequence coverage of the heavy chain. Comprehensive analysis of all of the HX-MS data from all peptides in all formulations would substantially diminish throughput without necessarily adding additional value for this application. As such, from this set of 360 peptides, a subset of 40 peptides was chosen for analysis. To generate this subset of peptides, a similar number of peptides were chosen from each domain of mAb-D, with some peptides exhibiting differences in deuterium accessibility in the presence of additives (based on screening studies) and others showing no differences in deuterium uptake. Peptides crossing domain boundaries were assigned to the domain belonging to the majority of its residues. The HX data were processed using HDEaminer software (Sierra Analytics, Modesto, CA). Difference plots for each peptide were generated by subtracting the mass of each peptide after labeling in CP control buffer from that of the peptide when labeled in the additive-containing buffer. For some figures, the y axis is displayed as “fractional uptake,” here defined as the uptake in Da divided by the number of residues in the peptide.

While HX-MS has the potential to be a useful tool for screening of additives for mAb stability effects, a barrier to this type of work is the propensity of differing excipient solutions to alter chemical exchange rates in HX experiments, rendering varying results from differing formulations. Recently, we have outlined a procedure to correct HX-MS data for these potential differences with minimal additional experimentation,<sup>18</sup> briefly, differences in chemical exchange rates in different formulations are determined using a short reporter peptide having the sequence YPI. Then a correction from the YPI data is determined that is used to empirically correct the HX data for differences in the intrinsic HX rate caused by the excipients, ensuring that any differences remaining are a function of protein dynamics.

## Results

### Screening of mAb-D for Stabilizing Additives by DSC, SEC, and MFI

Eight different additives were selected for evaluation in this work: trehalose, mannitol, methionine, arginine hydrochloride,

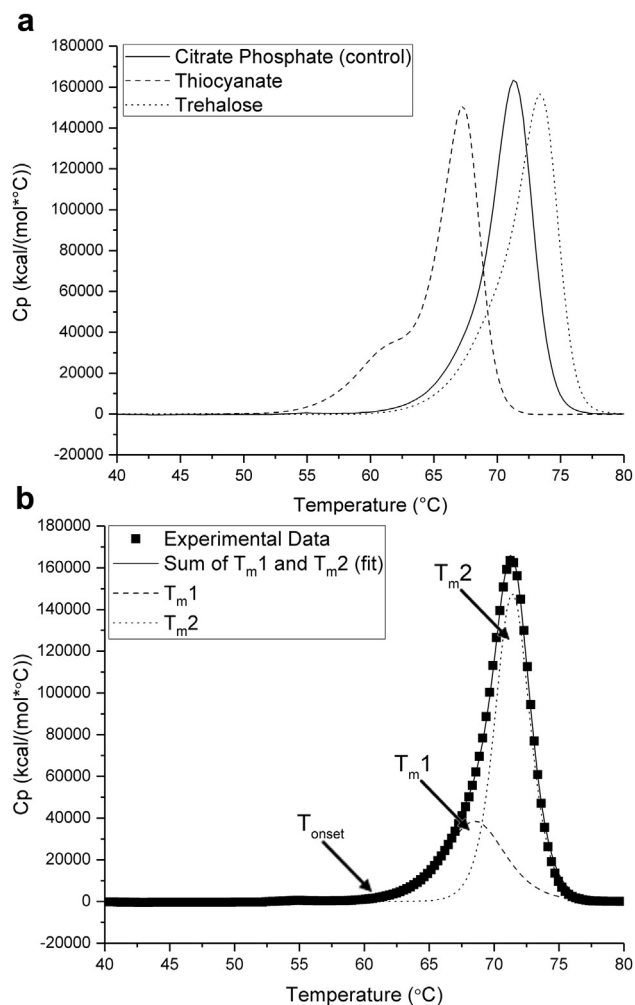


**Figure 1.** Differential scanning calorimetry studies show that additives affect conformational stability of mAb-D. (a) Representative DSC thermograms of mAb-D in CP buffer, pH 6.0 alone (control) and in the same buffer in the presence of thiocyanate and trehalose. (b) DSC data were fitted to a multistate model with 2 transitions, with the midpoints of each transition,  $T_{m1}$  and  $T_{m2}$ , identified. Also identified is the temperature at which the first transition begins,  $T_{onset}$ .

sodium sulfate, sodium thiocyanate, and Gdn-HCl. The additives cover different classes of pharmaceutical excipients including salts, amino acids, sugars, polyols, and detergents, or have well-established effects including both destabilization and stabilization of proteins.<sup>10</sup> As an initial step in better understanding the effect of these 8 different additives on the stability of an IgG4 mAb (mAb-D), differential scanning calorimetry was performed to evaluate their effects on the overall conformational stability of the mAb-D. Figure 1a shows representative DSC thermograms of mAb-D at pH 6.5 with 150-mM NaCl in the control buffer and with the control buffer containing a stabilizing and a destabilizing additive. The DSC thermograms were fitted to 2 thermal transitions ( $T_{m1}$  and  $T_{m2}$ ) as well as a thermal onset value ( $T_{onset}$ ) as shown in Figure 1b. The  $T_{m1}$ , corresponds to the C<sub>H2</sub> domain, and is likely to be important for the initiation of destabilization and aggregation as its unfolding occurs at the lowest temperature. Figure 2 shows the effect of the 8 additives on the thermal transitions of mAb-D at different solution pH values in the presence and absence of NaCl. It can be seen that thermal transition values of mAb-D trend somewhat higher at pH 7.4 compared with pH 6.5 and that the addition of NaCl had a minimal effect. In contrast, thiocyanate, guanidine, and arginine

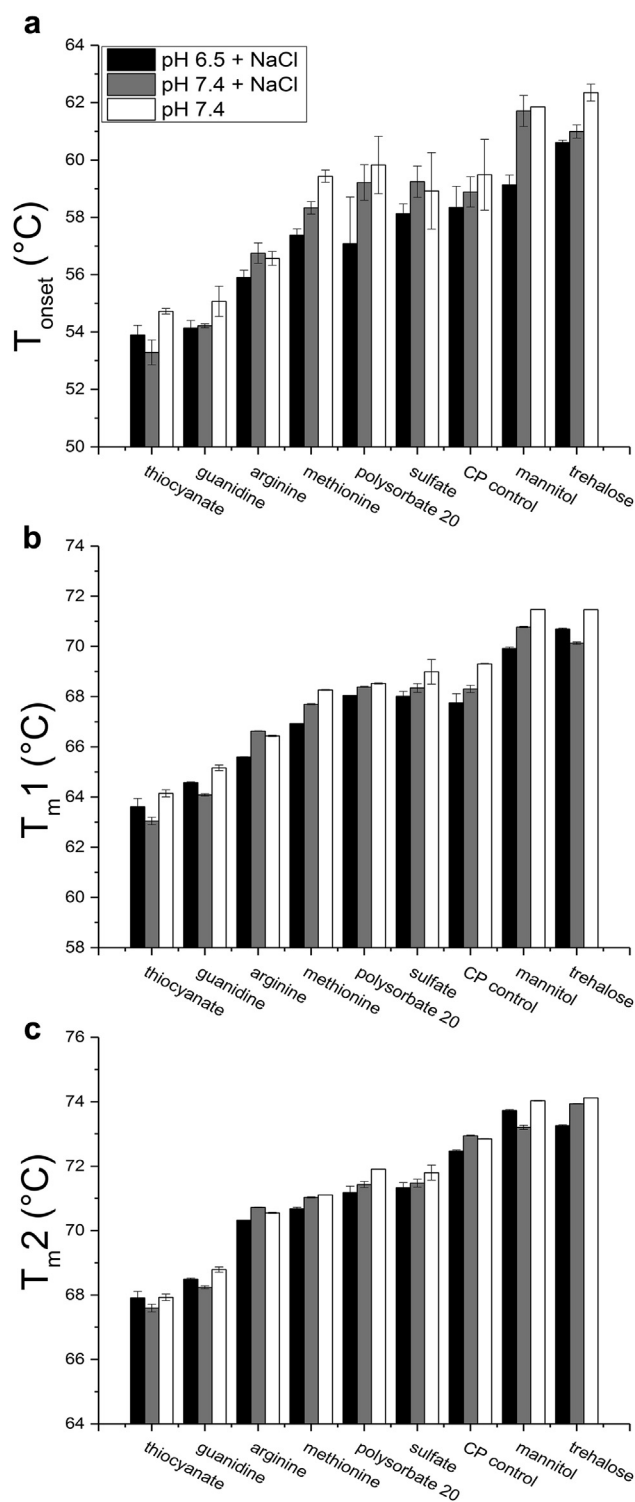


**Figure 2.** Effect of additives on the thermal transition values of mAb-D ( $T_{onset}$ ,  $T_{m1}$ , and  $T_{m2}$ ) as measured by DSC: (a)  $T_{onset}$ , (b)  $T_{m1}$ , and (c)  $T_{m2}$  values are shown. Additives are ordered from lowest to highest transition temperature of mAb-D, sorted by the average of the 3 different solution conditions. Samples were prepared in CP buffer at indicated pH values in the presence or absence of NaCl (pH 7.4) and different additives (see Materials and Methods section for concentrations). Error bars represent the sample standard deviation for triplicate measurements.

had a notable destabilizing effect, whereas mannitol and trehalose had a stabilizing effect. Methionine, PS20, and sodium sulfate had no major effects compared with the control mAb-D solution.

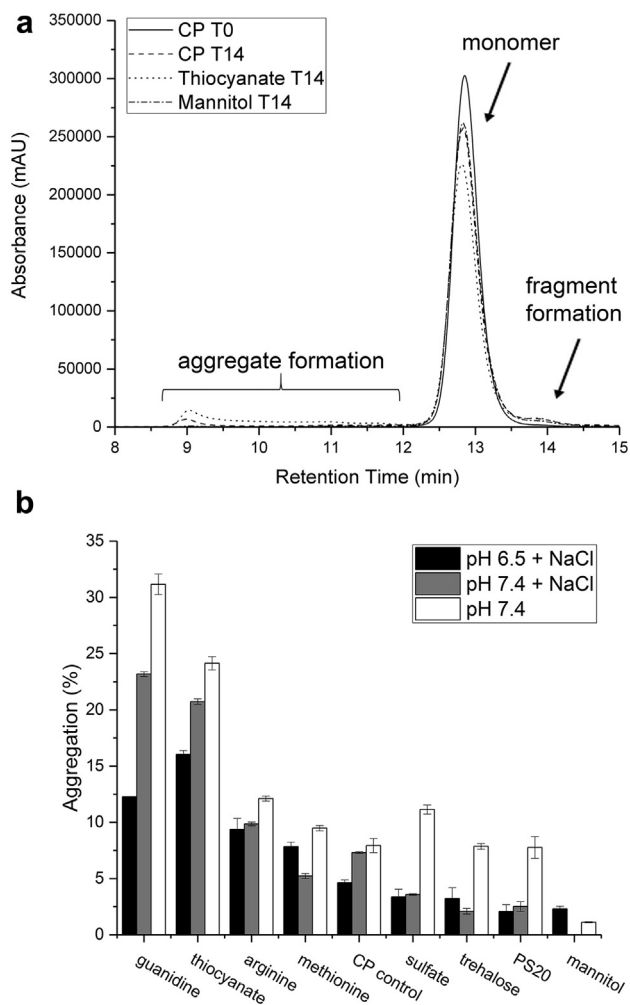


**Figure 3.** Effect of additives on total aggregate formation of mAb-D following incubation at 50°C for 14 days as measured by SEC. (a) Representative SEC profiles of mAb-D before and after accelerated stability study. (b) Rank ordering of additives from the highest to lowest percent aggregation of mAb-D in 3 different solution conditions. Samples were prepared in CP buffer at indicated pH values in the presence or absence of NaCl (pH 7.4) and different additives (see [Materials and Methods](#) section for concentrations). Error bars represent the sample standard deviation for triplicate measurements.

The effect of the same formulations on the aggregation propensity of mAb-D during storage at elevated temperatures was then evaluated by a combination of SEC and MFI analysis. SEC was performed on each of the mAb-D samples with and without various additives before and after incubation for 14 days at 50°C. [Figure 3](#) shows the effect of the additives on the total aggregate formation (soluble and insoluble aggregation) of mAb-D following heat stress. As shown in [Figure 3a](#) for mAb-D in control buffer alone, on heat stress, the formation of aggregate and fragment species occurs, as well as the loss of total area. The total amount of aggregation is defined as the sum of aggregate peaks (soluble aggregates) and the loss of total area (referred to here as insoluble aggregates; caused either by formation of aggregates too large to enter the column or nonspecific binding to the column which may be related to conformational changes). Also shown in [Figure 3a](#) is that additives in the control buffer can either alleviate or promote the formation of aggregates. [Figure 3b](#) shows the additives ranked by their propensity to promote aggregation. It can be seen that aggregation trends higher at pH 7.4 compared with pH 6.5, and that the absence

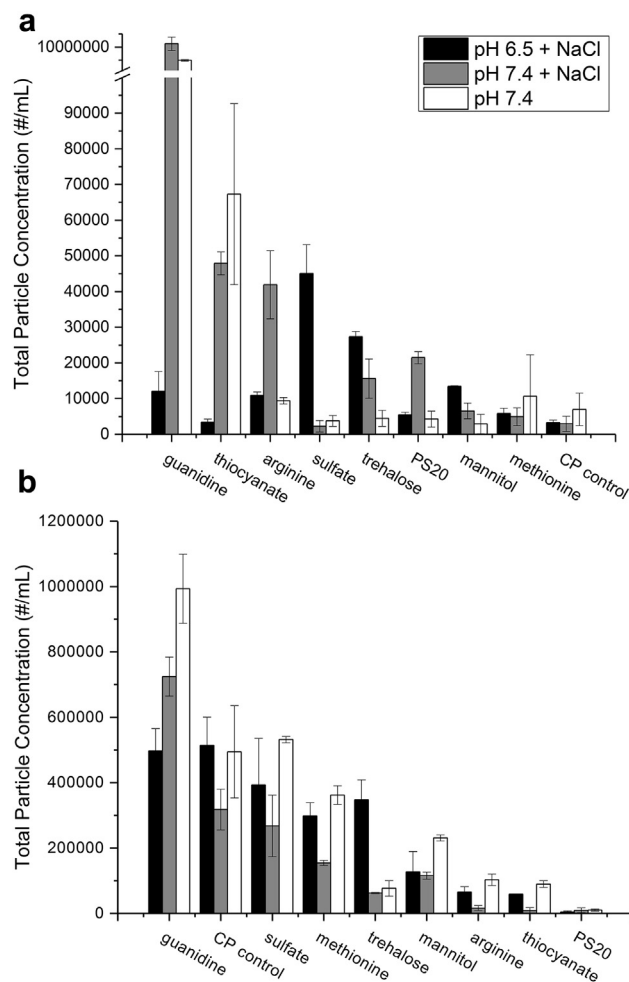


**Figure 4.** Effect of additives on subvisible particle formation by mAb-D as measured by MFI following incubation (a) at 50°C for 14 days, and (b) after stirring stress. Subvisible particles are defined as particle sized between 1 and 100  $\mu\text{m}$  in diameter. Additives are ordered from the highest to the lowest total particle concentration for mAb-D in 3 different solutions. Samples were prepared in CP buffer at indicated pH values in the presence or absence of NaCl (pH 7.4) and different additives (see [Materials and Methods](#) section for concentrations). Error bars represent the sample standard deviation for triplicate measurements.

of NaCl led to increased aggregation of mAb-D. The addition of thiocyanate, guanidine, and arginine had a notable destabilizing effect with large increases in aggregate formation. Mannitol had a stabilizing effect. Methionine, PS20, sodium sulfate, and trehalose had no major effects compared with the control mAb-D solution.

The same samples were also analyzed by MFI for formation of subvisible particles before and after incubation for 14 days at 50°C and after stirring stress. For both stresses, the total subvisible particle concentration before stress for each of the additive solutions was below 2500 particles/mL ([Supplemental Fig. S1a](#)). For conditions with 150-mM salt, the total particle concentrations of the mAb-D samples before stress were below 16,000 particles/mL for all additives, except sulfate, where total particle concentration before stress was higher, approximately  $10^5$  particles/mL (see [Supplemental Fig. S1b](#)). For samples without salt, the total particle concentrations before stress were higher but were still below 35,000 particles/mL for all samples ([Supplemental Fig. S1b](#)). Particle size distributions in mAb-D samples before stress, in general, have the highest concentration of particles in the smallest size bin and concentrations decrease with particle size ([Supplemental Fig. S2](#)). [Figure 4a](#) shows the effects of the additives on the total subvisible

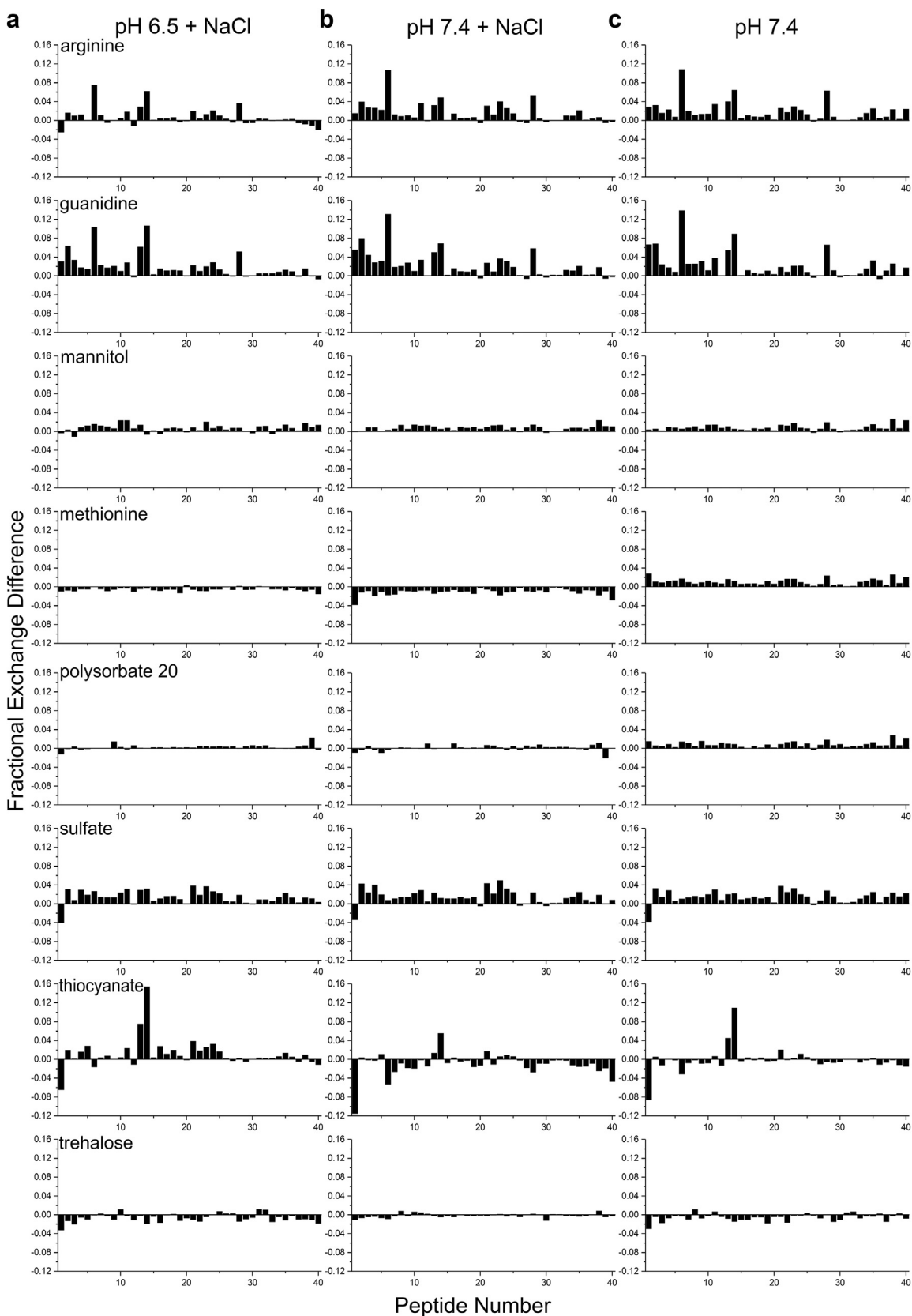


**Figure 5.** Difference plots exhibiting the differential fractional exchange by mAb-D in the presence of additives (vs. control buffer) in (a) CP buffer pH 6.5 with 150-mM NaCl, (b) CP buffer at pH 7.4 with 150-mM NaCl, and (c) CP buffer at pH 7.4 in the absence of salt, following correction for differences in chemical exchange rates (see [Materials and Methods](#) section). Fractional uptake is shown for all peptides; positive values indicate additive addition caused in increase in hydrogen exchange by the peptide segments, whereas negative values indicates decreased hydrogen exchange. Difference plots are shown for arginine, guanidine, mannitol, methionine, PS20, sulfate, thiocyanate, and trehalose.

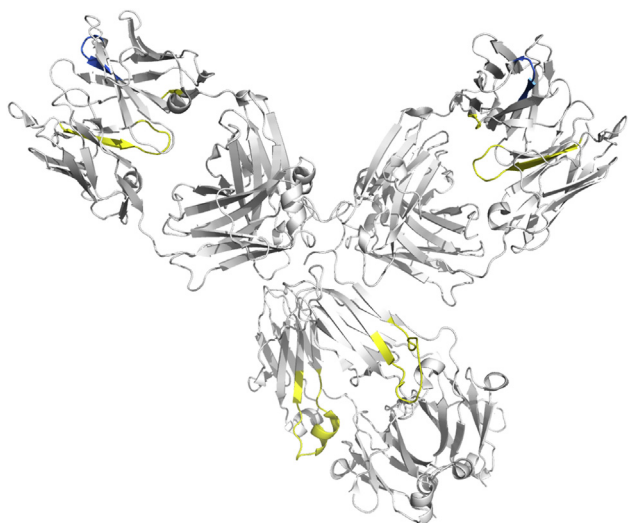


**Figure 6.** Homology model of mAb-D showing effects of selected additives on the local flexibility of mAb-D as measured by HX-MS. Regions shown in yellow (peptides 6, 13, 14, and 28; residues HC 112-115, HC 243-260, and LC 37-47) exhibited substantial increases in hydrogen exchange in the presence of thiocyanate, arginine, and guanidine. Regions in blue (peptide 1, HC 30-35) exhibited substantial decreases in hydrogen exchange in the presence of thiocyanate and sulfate. The mAb homology model is based on PDB 5DK3.<sup>21</sup>

particle formation by mAb-D following heat stress. Under these conditions, solution pH and NaCl had a complex effect on mAb-D subvisible particle formation with both stabilizing and destabilizing effects caused by the different additives. Thiocyanate, guanidine, arginine, and to a lesser extent sodium sulfate, had destabilizing effects leading to increases in subvisible particle formation. In contrast, methionine, trehalose, mannitol, and PS20 had no major effects compared with the control mAb-D solution with low concentrations of subvisible particles after stress. For most samples, although total particle concentrations increased on heat stress, the distribution of particles among the different size bins did not change (see [Supplemental Fig. S3](#)). Exceptions are the additives arginine and Gdn-HCl at pH 6.5 + NaCl, where the concentration of particles in the 5-10  $\mu\text{m}$  size bin increased relative to other bins (when compared to time 0) and guanidine at pH 7.4 without NaCl, where particle concentrations in the 5-10, 10-15, 15-25, and 25-40  $\mu\text{m}$  size bin increased relative to other bins when compared with time 0.

The effect of the same set of the 8 additives on the physical stability of mAb-D after stir stress was then evaluated. The results of MFI analysis of the number and size range of subvisible particles formed because of stirring are shown in [Figure 4b](#). Under stir stress conditions, solution pH and NaCl also had a complex effect on mAb-D subvisible particle formation with both stabilizing and destabilizing effects caused by different additives. Gdn-HCl had an effect on the stressed mAb-D samples leading to increases in subvisible particle formation. In contrast, sulfate and methionine had no notable effects compared with mAb-D control buffer. In addition, mAb-D solutions containing thiocyanate, arginine, trehalose, mannitol, and PS20 all displayed low concentrations of subvisible particles. For all samples, the particle size distributions on stir stress were altered compared with time 0, with particle concentrations in the smallest (2-5  $\mu\text{m}$ ) size bin increasing relative to other size bins.

#### Screening of Additives for Effects on mAb-D Local Flexibility by HX-MS

A peptide map was developed for mAb-D consisting of 360 peptides with 97% sequence coverage of the light chain and 98%

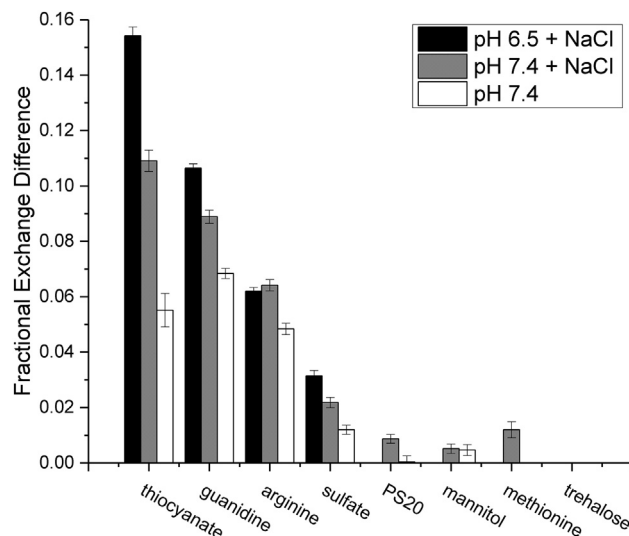


**Figure 7.** Fractional exchange differences in the mAb-D C<sub>H2</sub> aggregation hotspot peptide (heavy chain residues 250-260) in the presence of the indicated additives. Data are shown for mAb-D at pH 6.5 with 150-mM NaCl and pH 7.4 with and without 150-mM NaCl following correction for differences in chemical exchange rates (see [Materials and Methods](#) section). Additives are ordered by the average differential deuterium uptake averaged among the 3 conditions from greatest to least. Error bars represent the sample standard deviation for triplicate measurements propagated over the differences.

sequence coverage of the heavy chain. To reduce analysis load, a subset of 40 peptides were chosen for analysis such that a similar number of peptides covered each domain of mAb-D. HX was then measured for mAb-D in 5-mM CP and mAb-D in 5-mM CP with each 1 of the 8 additives, at the salt and pH conditions described previously. After the reaction was quenched at different exchange times, peptic peptides were generated and analyzed by LC-MS to determine deuterium uptake. A chemical exchange correction factor was established for all solution conditions as described in methods.<sup>18</sup> [Figure 5a-5c](#) show plots of the difference (following additive correction) between HX by mAb-D with additives minus mAb-D in control buffers.

[Figure 5](#) demonstrates that additives can have a substantial effect on HX results with mAb-D. For example, the additives arginine, guanidine, sulfate, and thiocyanate caused substantial increases in HX in many peptide segments, relative to mAb-D in the corresponding control buffer, indicating increases in backbone flexibility. Concurrent with these substantial increases in flexibility for specific peptide segments was a trend of small increases in flexibility in the majority of peptide segments for those same additives except thiocyanate. Mannitol, methionine (for pD 7.4 with NaCl), and PS20 (for pD 6.5 + NaCl and pD 7.4 + NaCl) caused slight global increases in flexibility without the substantial localized increases that were observed in the presence of arginine, guanidine, sulfate, and thiocyanate. The opposite effect was also noted for some additives, with a global decrease in flexibility for methionine (pD 6.5 + NaCl and pD 7.4) and trehalose. In general, increased pH (comparing left column to middle column) had no notable effect on flexibility with the exception of methionine where increased pH caused a slight global increase in flexibility and thiocyanate where increased pH caused a slight global decrease in flexibility. Addition of salt (comparing right column to middle column) had no notable effect for arginine, guanidine, mannitol, and sulfate, while resulting in a slight increase in flexibility for methionine, PS20, and thiocyanate, and a slight decrease in flexibility for trehalose. For

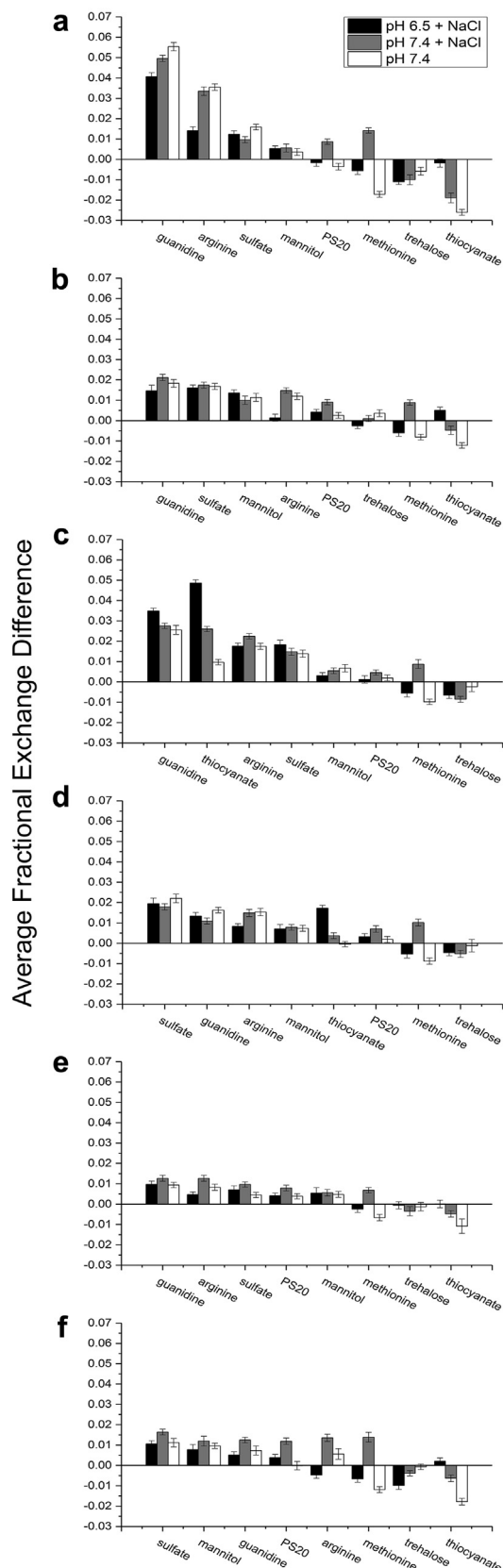


**Figure 8.** The effect of additives on the domain-averaged fractional exchange differences in mAb-D domains. Data are shown for the (a)  $V_H$ , (b)  $C_{H1}$ , (c)  $C_{H2}$ , (d)  $C_{H3}$ , (e)  $V_L$ , and (f)  $C_L$  domains of mAb-D in the presence of the indicated additive (vs. control buffer) at pH 6.5 with 150-mM NaCl and pH 7.4 with and without 150-mM NaCl following correction for differences in chemical exchange rates (see [Materials and](#)

visualization of these HX observations, the most substantial additive effects on local flexibility of mAb-D were mapped onto a homology model of the antibody (based on PDB 5DK3<sup>21</sup>) displayed in [Figure 6](#).

## Discussion

The main goal of this study was to correlate the HX data collected with mAb-D in the presence of various additives with both conformational stability data (DSC) and the propensity of mAb-D to form aggregates and particulates over time (as measured by an accelerated stability study combined with SEC and MFI analysis). We aimed to determine what aspects of mAb-D stability (from a pharmaceutical perspective) can be most directly reported on by local flexibility analysis from HX-MS, and to evaluate whether a streamlined version of HX-MS can serve as a useful screening technique to identify stabilizing excipients. If adequate correlates can be found, HX-MS may serve as a useful technique to predict aspects of mAb storage stability in different solutions and thus has the potential (given additional correlations with more comprehensive stability data sets as part of future work) to be used as an alternative to accelerated stability studies.<sup>22</sup> To this end, as a first step, we focused on various approaches to analyze the HX-MS data generated with mAb-D in the presence of various additives (e.g., commonly used pharmaceutical excipients as well as control additives known to destabilize proteins) to provide an overall description of the trends (in terms of excipient effects) that can be more easily compared with mAb-D stability data collected by more traditional approaches, as outlined below.

### Traditional Additive Screening Studies With mAb-D Using DSC, SEC, and MFI

Results from DSC studies ([Fig. 2](#)) reveal that mAb-D is conformationally destabilized in the presence of guanidine, thiocyanate, and arginine, listed from greatest to least destabilizer. In addition, trehalose proved to be the most notable conformational stabilizer of mAb-D. In general, increased pH (comparing blue through orange bars) resulted in a trend (although within error) toward an increase in thermal stability for mAb-D in all additive solutions, with the exception of thiocyanate and guanidine, where increased pH slightly decreased thermal stability (also within error). Addition of salt (comparing black and gray bars) in general caused a slight decrease in thermal stability for mAb-D in all additive solutions (within error) with the exception of arginine, where thermal stability slightly increased (within error) on addition of salt.

Results from SEC studies of aggregation after heat stress ([Fig. 3](#)) reveal the same trend, with mAb-D exhibiting the greatest increase in percent aggregation in the presence of guanidine, thiocyanate, and arginine, listed from greatest aggregation to least. In addition, results on subvisible particle formation from MFI studies ([Fig. 4](#)) following heat stress further confirm this trend, with mAb-D in the presence of guanidine, thiocyanate, and arginine showing the greatest total particle concentrations, listed in order from greatest total particle concentration to least. Trehalose was not a significant stabilizer in aggregation due to heat stress studies. Results from SEC

([Methods](#) section). Fractional uptake difference was averaged over the 5 peptides (peptides 1–4 and 6 for  $V_H$ , 8–12 for  $CH1$ , 13, 14, and 16–18 for  $CH2$ , 21–25 for  $CH3$ , 27–31 for  $V_L$ , and 34, 35, and 38–40 for  $CL$ ) showing the greatest magnitude of effect in the data set (the same group of 5 for all additives and conditions). Additives are ordered by the average differential deuterium uptake averaged among the 3 conditions from greatest to least. Error bars represent the sample standard deviation for triplicate measurements propagated over the average of the differences.



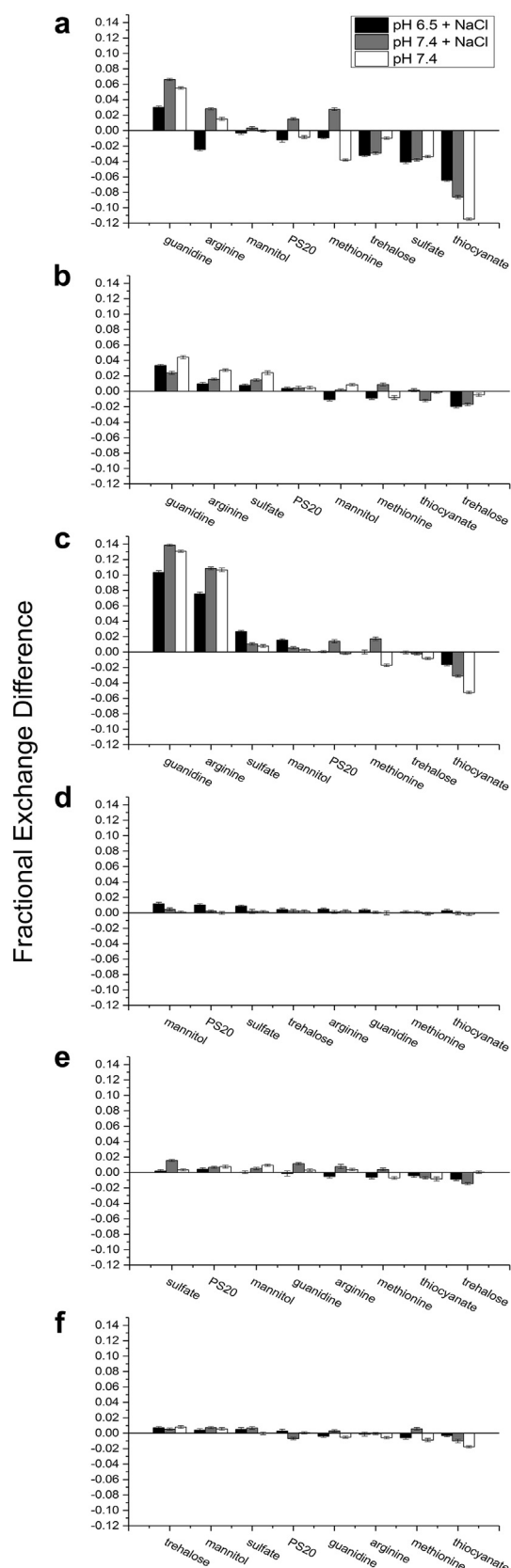


**Figure 9.** Fractional exchange differences in the CDR regions of mAb-D in presence of various additives. Data are shown for (a, peptide 1) CDR-H1, (b, peptide 3) CDR-H2, (c, peptide 6) CDR-H3, (d, peptide 27) CDR-L1, (e, peptide 29) CDR-L2, and (f, peptide 31) CDR-L3 in the presence of the indicated additive (vs. control buffer) at pH 6.5 with 150-mM NaCl and pH 7.4 with and without 150-mM NaCl following correction for

and MFI studies of aggregation after heat stress reveal that increased solution pH values (comparing blue to gray bars, Figs. 3b and 4a) resulted in a substantial increase in aggregation for destabilizing additives, yet values were within error for stabilizing additives. Addition of salt (comparing black and gray bars) resulted in a substantial decrease in mAb-D aggregation due to heat stress for all additive solutions, both stabilizing and destabilizing. These results indicate that mAb-D is less colloidal stable at pH values above the pI of mAb-D (~7.07, estimated based on sequence) where mAb-D is net negatively charged, and that addition of salt alleviates this colloidal instability, perhaps by screening of electrostatic interactions.

In summary, the results from heat stress of mAb-D in the presence of the 8 additives indicate that conformational destabilization is likely an important step in the pathway to aggregation due to heat stress for mAb-D. In the first step of one of the main aggregation pathways of mAbs proposed by Roberts et al.,<sup>23,24</sup> and confirmed by others,<sup>25</sup> the native monomers become partially unfolded and begin to associate into loose clusters. In the second step, within these clusters the now exposed aggregation hotspots can align and lead to the formation of irreversible aggregates. It is likely that the DSC results report on this first conformational destabilization step thus its apparent correlation with aggregation due to heat stress.

In general, the results of aggregation due to stir stress (Fig. 4b) do not correlate with DSC results (in contrast to the results described above for heat stress). Most notably, the additives thiocyanate and arginine, while significant destabilizers in DSC (Fig. 2) and aggregation due to heat stress (Figs. 3b and 4a) studies, are significant stabilizers for aggregation due to stir stress. These results indicate that aggregation due to stir stress does not follow the same pathway as aggregation due to heat stress. It is likely that the pathway responsible for aggregation due to stir stress instead involves unfolding and nucleation on the liquid-solid or liquid-air interfaces,<sup>26</sup> thus the ability of surfactants such as PS20 and zwitterions such as arginine to act as stabilizers.

#### Additive Screening Studies With mAb-D Using HX-MS

To correlate these results with the HX data, we must also treat the HX data to obtain an overall trend. Here we do so by reducing the dimensionality of the HX data in several ways. First, we restrict our view to a  $C_H2$  aggregation hotspot region identified previously in our laboratory in IgG1 mAbs<sup>27</sup> (Fig. 7). This region covers residues 241-251 in the heavy chain and contains several hydrophobic residues that pack against glycans in the structure of IgG1 mAbs. This region corresponds to residues 250-260 for mAb-D. In general, the  $C_H2$  peptide was significantly more flexible in the presence of thiocyanate, guanidine, arginine, and sulfate than in control buffer, listed in that order from greatest to least increase. In comparison to the control buffer alone, PS20, mannitol, and methionine had no effect within experimental error. Finally, the  $C_H2$  peptide was significantly more rigid in the presence of trehalose. This additive trend most closely matches that of the conformational stability of mAb-D as measured by DSC, suggesting that HX in this case is reporting most directly on conformational stability. This trend also matches that of mAb-D aggregation due to heat stress, and likely this correlation exists for the reason mentioned previously, that conformational destabilization is an important step in the pathway

differences in chemical exchange rates (see Materials and Methods section). Additives are ordered by the average differential deuterium uptake averaged among the 3 conditions from greatest to least. Error bars represent the sample standard deviation for triplicate measurements, propagated over the difference.

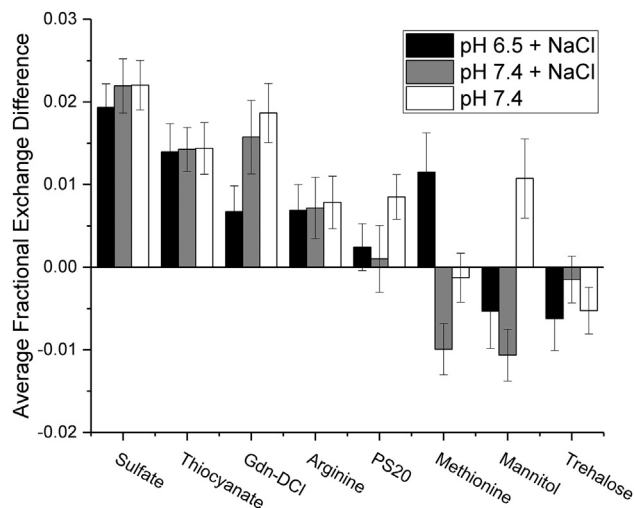


**Figure 10.** The effect of additives on the fractional exchange difference averaged across all peptides in mAb-D. Data are shown for mAb-D in the presence of the indicated additive (vs. control buffer) at pH 6.5 with 150-mM NaCl and pH 7.4 with and without 150-mM NaCl following correction for differences in chemical exchange rates (see [Materials and Methods](#) section). Additives are ordered by the average fractional exchange difference averaged among the 3 conditions from greatest to least. Error bars represent the sample standard deviation for triplicate measurements, propagated over the average of the differences.

to aggregation due to heat stress for mAb-D, a common aggregation pathway for mAbs.<sup>24,28</sup>

We also averaged the HX data over the 5 peptides from each domain with the greatest magnitude (absolute value) of fractional exchange difference, chosen from among the 40 peptides seen in [Figure 5](#) ([Fig. 8](#)). No trends were found in the effects of additives matching those seen in conformational stability and aggregation due to heat stress, with the exception of the C<sub>H2</sub> domain. The trend in the C<sub>H2</sub> domain explicable by the influence of the C<sub>H2</sub> aggregation hotspot peptide discussed previously.

In addition, we restricted our view of the HX data to one peptide (chosen from the subset of 40) spanning each

complementarity-determining region (CDR) region ([Fig. 9](#)), as well as to the average HX difference over the whole protein ([Fig. 10](#)). No correlations were found when examining the HX data from the CDR regions of mAb-D ([Fig. 9](#)) or when examining the HX data averaged over the whole protein ([Fig. 10](#)). This result may seem at odds with studies where the nature of the CDR loops are found to be important in the aggregation pathway of a mAb<sup>29</sup>; however, it is possible that for mAb-D, the composition of the CDR loops are not prone to induce aggregation, and thus the observed C<sub>H2</sub> destabilization (observed by HX within an aggregation “hotspot”, residues 250–260 for mAb-D) is the rate-limiting step in the aggregation pathway for this particular mAb. The effects of additives on the whole protein's average flexibility can be seen in [Figure 10](#), showing fractional uptake averaged among all peptides. The overall trends in the HX are that guanidine, sulfate, arginine, mannitol, and PS20 caused an increase in average global hydrogen exchange across the entire protein. Both thiocyanate and methionine had no effect on the average global exchange, whereas trehalose caused a decrease in average global exchange.

In contrast to heat stress, where a good correlation was observed between HX of the aggregation hotspot (and entire C<sub>H2</sub> domain) and mAb-D physical stability, no such correlation was found between HX and aggregation due to stir stress. Likely this is because the aggregation pathway for stir stress is an interfacial phenomenon that does not involve steps that HX-MS can report on directly. It has been established that mAbs often follow differing aggregation pathways depending on the stress applied.<sup>28</sup> Here, an apparent trend is that amphipathic molecules capable of acting as surfactants (e.g., PS20) tend to be stabilizers in aggregation due to stir stress, indicating that the pathway for aggregation due to stir stress likely involves accumulation of protein at the air/water interface, another common pathway.<sup>28</sup>

Results from averaged HX-MS results and biophysical studies, as a function of heat and stir stresses, are summarized in [Figure 11](#), where additives are colored based on HX-MS results for the C<sub>H2</sub> aggregation hotspot peptides. In general, additives that promote flexibility in a hotspot peptide (yellow) of mAb-D tend to be destabilizing in terms of conformation (measured by DSC) and aggregation propensity during storage at elevated temperatures (as

a	HX-MS			b	Biophysical (Heat Stress)			c	Biophysical (Stir Stress)
	Hotspot Peptide	C <sub>H2</sub> Domain	Whole Protein		DSC	SEC	MFI		MFI
Increased Flexibility	Guanidine	Guanidine	Guanidine	Destabilizing	Guanidine	Guanidine	Guanidine	Destabilizing	Guanidine
	Thiocyanate	Thiocyanate	Mannitol		Thiocyanate	Thiocyanate	Thiocyanate		
	Arginine	Arginine	Arginine		Arginine	Arginine	Arginine		
	Sulfate	Sulfate	Sulfate						
Within Error of Control			PS20	Within Error of Control	Sulfate	Sulfate	Sulfate	Within Error of Control	Sulfate
	Methionine	Methionine	Thiocyanate		Methionine	Methionine	Methionine		Methionine
	Mannitol	Mannitol	Methionine		PS20	PS20	PS20		
Reduced Flexibility				Stabilizing		Trehalose	Trehalose	Stabilizing	Trehalose
						Mannitol	Mannitol		Mannitol
								Thiocyanate	
								PS20	

**Figure 11.** Generalized conclusions from biophysical and HX-MS studies of the effect of additives on mAb-D physical stability profile and local flexibility in presence of different additives. (a) In the first section, additives are placed in 1 of 3 categories based on conclusions from HX-MS data; increased flexibility, within error of control, and reduced flexibility. (b, c) In subsequent sections, additives are placed in 1 of 3 categories based on conclusions from biophysical data; destabilizing, within error of control, and stabilizing. Additives are colored based on HX-MS results for hotspot peptide (first column) and retained in other columns to highlight commonalities (e.g., guanidine ranking highly in all studies).

measured by SEC). The exception to this trend is sulfate, which caused increased flexibility in HX-MS studies in the hotspot region of mAb-D, but was not observed to be a destabilizer in the physical stability studies. In the HX-MS studies, sulfate increased flexibility to a lesser extent than guanidine, thiocyanate, or arginine. It is possible that the smaller increase in flexibility is not sufficient to destabilize mAb-D during storage, or that the destabilization effect would be revealed only with longer incubation times. It is also possible that the destabilization by sulfate is more complex phenomena given that sulfate is a divalent anion (e.g., charge shielding effects). In contrast, no such consistent trend between additive effects on mAb-D as measured by HX-MS, DSC, and SEC studies were observed when stirring is the stress.

## Conclusion

The ability to directly compare data gathered for mAb-D in different solutions (containing either commonly used pharmaceutical excipients or control additives known to destabilize proteins) allowed us to evaluate correlations between HX-MS data and other mAb-D stability data sets (e.g., conformational stability using DSC and accelerated stability studies monitoring protein aggregation by SEC and MFI using both temperature and agitation as stresses). The effect of additives on the relative local flexibility of specific C<sub>H2</sub> peptide segments within mAb-D correlated well with conformational stability and aggregation propensity under accelerated stability conditions involving heat stress, confirming the C<sub>H2</sub> aggregation hotspot, identified in previous work with IgG1 mAbs,<sup>27</sup> with this IgG4 mAb. There were, however, no convincing correlations between HX-MS data and stirring stress for additive effects on the stability of mAb-D. These results indicate that potentially useful correlations between HX-MS data (using minimal material and a streamlined data analysis approach focusing on key peptide segments) with accelerated and real-time stability data to identify stabilizing additives as part of formulation development will be dependent on a particular mAbs degradation pathway(s) and the type of stresses used for the additive screening studies. To this end, using a variety of different mAbs, additional correlations of HX readouts in various formulations with more comprehensive accelerated and real-time stability data sets will need to be generated as part of future work.

## Acknowledgments

The KU authors acknowledge Medimmune, LLC for funding support and the NIH Biotechnology Training grant 5T32GM008359-25 for support of Samantha Pace. An equipment loan from Agilent Technologies is gratefully acknowledged.

## References

- Reichert JM. Antibody-based therapeutics to watch in 2011. *MAbs*. 2011;3(1):76-99.
- Reichert JM. Antibodies to watch in 2014. *MAbs*. 2014;6(1):5-14.
- Kamerzell TJ, Middaugh CR. The complex inter-relationships between protein flexibility and stability. *J Pharm Sci*. 2008;97(9):3494-3517.
- Majumdar R, Middaugh CR, Weis DD, Volkin DB. Hydrogen-deuterium exchange mass spectrometry as an emerging analytical tool for stabilization and formulation development of therapeutic monoclonal antibodies. *J Pharm Sci*. 2015;104(2):327-345.
- Kessler H, Mronga S, Müller G, Moroder L, Huber R. Conformational analysis of a IgG1 hinge peptide derivative in solution determined by NMR spectroscopy and refined by restrained molecular dynamics simulations. *Biopolymers*. 1991;31(10):1189-1204.
- Nelson AL, Dhimolea E, Reichert JM. Development trends for human monoclonal antibody therapeutics. *Nat Rev Drug Discov*. 2010;9(10):767-774.
- Cohen-Solal JFG, Cassard L, Fridman W, Sautès-Fridman C. Fc  $\gamma$  receptors. *Immunol Lett*. 2004;92(3):199-205.
- Raghavan M, Bjorkman PJ. Fc receptors and their interactions with immunoglobulins. *Annu Rev Cell Dev Biol*. 1996;12:181-220.
- Ravetch JV, Bolland S. IgG Fc receptors. *Annu Rev Immunol*. 2001;19:275-290.
- Kamerzell TJ, et al. Protein-excipient interactions: mechanisms and biophysical characterization applied to protein formulation development. *Adv Drug Deliv Rev*. 2011;63(13):1118-1159.
- Chaudhuri R, Cheng Y, Middaugh CR, Volkin DB. High-throughput biophysical analysis of protein therapeutics to examine interrelationships between aggregate formation and conformational stability. *AAPS J*. 2014;16(1):48-64.
- Maddux NR, Joshi SB, Volkin DB, Ralston JP, Middaugh CR. Multidimensional methods for the formulation of biopharmaceuticals and vaccines. *J Pharm Sci*. 2011;100(10):4171-4197.
- Alsenaidy MA, Jain NK, Kim JH, Middaugh CR, Volkin DB. Protein comparability assessments and potential applicability of high throughput biophysical methods and data visualization tools to compare physical stability profiles. *Front Pharmacol*. 2014;5:39.
- Yan Y, Wei H, Jusuf S, et al. Mapping the binding interface in a noncovalent size variant of a monoclonal antibody using native mass spectrometry, hydrogen-deuterium exchange mass spectrometry, and computational analysis. *J Pharm Sci*. 2017;106(11):3222-3229.
- Huang RY, Jacob RE, Krystek SR, et al. Characterization of aggregation propensity of a human Fc-fusion protein therapeutic by hydrogen/deuterium exchange mass spectrometry. *J Am Soc Mass Spectrom*. 2017;28(5):795-802.
- Li J, Wei H, Krystek SR, et al. Mapping the energetic epitope of an antibody/interleukin-23 interaction with hydrogen/deuterium exchange, fast photochemical oxidation of proteins mass spectrometry, and alanine shave mutagenesis. *Anal Chem*. 2017;89(4):2250-2258.
- Li KS, Chen G, Mo J, et al. Orthogonal mass spectrometry-based footprinting for epitope mapping and structural characterization: the IL-6 receptor upon binding of protein therapeutics. *Anal Chem*. 2017;89(14):7742-7749.
- Toth RT, Mills BJ, Joshi SB, et al. Empirical correction for differences in chemical exchange rates in hydrogen exchange-mass spectrometry measurements. *Anal Chem*. 2017;89(17):8931-8941.
- Glasoe PK, Long FA. Use of glass electrodes to measure acidities in deuterium oxide 1,2. *J Phys Chem*. 1960;64(1):188-190.
- Arora J, Joshi SB, Middaugh CR, Weis DD, Volkin DB. Correlating the effects of antimicrobial preservatives on conformational stability, aggregation propensity, and backbone flexibility of an IgG1 monoclonal antibody. *J Pharm Sci*. 2017;106(6):1508-1518.
- Scapin G, Yang X, Prosser WW, et al. Structure of full-length human anti-PD1 therapeutic IgG4 antibody pembrolizumab. *Nat Struct Mol Biol*. 2015;22(12):953-958.
- Thiagarajan G, Semple A, James JK, Cheung JK, Shameem M. A comparison of biophysical characterization techniques in predicting monoclonal antibody stability. *MAbs*. 2016;8(6):1088-1097.
- Roberts CJ. Protein aggregation and its impact on product quality. *Curr Opin Biotechnol*. 2014;30:211-217.
- Roberts CJ. Therapeutic protein aggregation: mechanisms, design, and control. *Trends Biotechnol*. 2014;32(7):372-380.
- Kalonia C, Toprani VM, Toth RT, et al. Effects of protein conformation, apparent solubility, and protein-protein interactions on the rates and mechanisms of aggregation for an IgG1 monoclonal antibody. *J Phys Chem B*. 2016;120(29):7062-7075.
- Perevozchikova T, Nanda H, Nesta DP, Roberts CJ. Protein adsorption, desorption, and aggregation mediated by solid-liquid interfaces. *J Pharm Sci*. 2015;104(6):1946-1959.
- Manikwar P, Majumdar R, Hickey JM, et al. Correlating excipient effects on conformational and storage stability of an IgG1 monoclonal antibody with local dynamics as measured by hydrogen/deuterium-exchange mass spectrometry. *J Pharm Sci*. 2013;102(7):2136-2151.
- Amin S, Barnett GV, Pathak JA, Roberts CJ, Sarangapani PS. Protein aggregation, particle formation, characterization and rheology. *Curr Opin Colloid Interface Sci*. 2014;19(5):438-449.
- Wang X, Das TK, Singh SK, Kumar S. Potential aggregation prone regions in biotherapeutics: a survey of commercial monoclonal antibodies. *MAbs*. 2009;1(3):254-267.